The Company of Biologists

RESEARCH ARTICLE

Dynamic body acceleration as a proxy to predict the cost of locomotion in bottlenose dolphins

Austin S. Allen[1],*, Andrew J. Read[1], K. Alex Shorter[2], Joaquin Gabaldon[3], Ashley M. Blawas[1], Julie Rocho-Levine[4] and Andreas Fahlman[5,6]

ABSTRACT

Estimates of the energetic costs of locomotion (COL) at different activity levels are necessary to answer fundamental eco-physiological questions and to understand the impacts of anthropogenic disturbance to marine mammals. We combined estimates of energetic costs derived from breath-by-breath respirometry with measurements of overall dynamic body acceleration (ODBA) from biologging tags to validate ODBA as a proxy for COL in trained common bottlenose dolphins (*Tursiops truncatus*). We measured resting metabolic rate (RMR); mean individual RMR was 0.71–1.42 times that of a similarly sized terrestrial mammal and agreed with past measurements that used breath-by-breath and flow-through respirometry. We also measured energy expenditure during submerged swim trials, at primarily moderate exercise levels. We subtracted RMR to obtain COL, and normalized COL by body size to incorporate individual swimming efficiencies. We found both mass-specific energy expenditure and mass-specific COL were linearly related with ODBA. Measurements of activity level and cost of transport (the energy required to move a given distance) improve understanding of the COL in marine mammals. The strength of the correlation between ODBA and COL varied among individuals, but the overall relationship can be used at a broad scale to estimate the energetic costs of disturbance and daily locomotion costs to build energy budgets, and investigate the costs of diving in free-ranging animals where bio-logging data are available. We propose that a similar approach could be applied to other cetacean species.

KEY WORDS: Swimming, Energetics, Biologging, Respirometry, Cetacean, *Tursiops truncatus*

INTRODUCTION

Animals expend energy in four physiological processes: maintenance, growth, reproduction and physical activity. One component of physical activity is movement (Gleiss et al., 2011). The energy allocated to movement, also termed the cost of locomotion (COL), can vary greatly depending on life history and activity level, and is the primary source of energy use in many vertebrates (Karasov, 1992). For example, cheetahs

(*Acinonyx jubatus*) may expend up to 100 W kg^{-1} during a sprint (Wilson et al., 2013), although the short duration of such activity means that sprints have a negligible impact on their daily energy budget (Scantlebury et al., 2014). In contrast, African wild dogs (*Lycaon pictus*) spend hours hunting at a lower energetic cost (35 W kg^{-1}), so this activity comprises a large portion of their daily energy budget (Gorman et al., 1998). Because energy expenditure is linked to fitness (Grémillet et al., 2018), estimates of COL underpin many ecological questions, including understanding the effects of anthropogenic impacts. For example, COL can help parameterize population consequences of disturbance (PCoD) models to quantify the impacts of cumulative, sublethal threats to marine mammals (Pirotta et al., 2018).

Several methods exist to estimate COL, although there is considerable debate over which method is best for different species and contexts. The doubly labeled water method uses labeled isotopes to estimate field metabolic rate (FMR) and can be linked to activity budgets to estimate COL (Jeanniard-du-Dot et al., 2017b). Although doubly labeled water has been used in two cetacean species (Costa et al., 2013; Rimbach et al., 2021; Rojano-Doñate et al., 2018), proper validation and logistical considerations make this method difficult to use with large, free-ranging mammals (Butler et al., 2004; Speakman, 1997). Respiration has also been used as a proxy for FMR (Sumich, 2021; Villegas-Amtmann et al., 2015), although variation in tidal volume and end-tidal gas concentrations can cause significant uncertainty, especially over short time scales (Fahlman et al., 2016; Roos et al., 2016). Owing to the logistical constraints of working with large, aquatic, air-breathing animals, published estimates of COL are more limited for marine mammals than for terrestrial taxa.

Recent advances in biologging technology have facilitated the development of two additional proxies for COL: heart rate and activity (Wilmers et al., 2015; Wilson et al., 2020). In many taxa, heart rate correlates with energy use (Green, 2011). However, marine mammals exhibit cardiorespiratory changes related to submergence that are believed to be under conditioned control in at least some species (Fahlman et al., 2020; McDonald et al., 2018). Therefore, marine mammals may be able to temporally decouple heart rate from energy expenditure (Williams et al., 2017). An additional challenge to using heart rate as an energetic proxy is the logistical complexity of attaching external heart rate monitors to free-ranging marine mammals. In contrast, some short-duration, high-resolution archival tags include tri-axial accelerometers that can be used to measure activity level. Activity level (e.g. stroke rate, body acceleration, speed) has been used to predict fine-scale COL in many taxa, including marine mammals (Wilson et al., 2020).

Activity metrics generated from biologging tags include stroke frequency, dynamic body acceleration (DBA) calculated either as vectorial (VeDBA) or as an overall measure (ODBA; Qasem et al., 2012; Wilson et al., 2020, 2006), and, less frequently, speed (Gabaldon et al., 2019). When most of the measured acceleration is

[1]Duke University Marine Lab, Beaufort, NC 28516, USA. [2]Mechanical Engineering, University of Michigan, Ann Arbor, MI 48109, USA. [3]Robotics Institute, University of Michigan, Ann Arbor, MI 48109, USA. [4]Dolphin Quest Oahu, Honolulu, HI 96816, USA. [5]Fundación Oceanogràfic de la Comunitat Valenciana, Research Department, Valencia 46005, Spain. [6]Kolmården wildlife park, Kolmården, SE-618 92, Sweden.

*Author for correspondence (austin.allen@duke.edu)

A.S.A., 0000-0002-5165-8879; J.G., 0000-0003-3775-6154; A.M.B., 0000-0003-4109-9003; A.F., 0000-0002-8675-6479

List of symbols and abbreviations

BMR	basal metabolic rate
COL	cost of locomotion (W)
COL_{norm}	normalized cost of locomotion (W/η)
COT	cost of transport (J kg^{-1} m^{-1})
DBA	dynamic body acceleration
$D_{SS,Lap}$	duration submerged during steady-state (min)
$D_{SS,Station}$	duration at station (not submerged) during steady-state (min)
FMR	field metabolic rate
ICC	intraclass correlation
LD	mean individual lap distance (m) travelled
M_b	body mass (kg)
ODBA	overall dynamic body acceleration
PCoD	population consequences of disturbance
RMR	resting metabolic rate (ml O_2 min^{-1})
VeDBA	vectorial sum of the dynamic body acceleration
V_{CO_2}	volume of CO_2 consumed (ml CO_2)
$\dot{V}_{CO_2}$	rate of CO_2 consumption (ml CO_2 min^{-1})
V_{O_2}	volume of O_2 consumed (ml O_2)
$V_{O_2,SS}$	volume of O_2 consumed during steady-state (ml O_2)
$\dot{V}_{O_2}$	rate of O_2 consumption (ml O_2 min^{-1})
$\dot{V}_{O_2,average}$	mean rate of O_2 consumption (ml O_2 min^{-1}) during lap and station combined
$\dot{V}_{O_2,sCOL}$	mass-specific rate of O_2 consumption over resting values (ml O_2 kg^{-1} min^{-1})

due to mechanical work performed by locomotor muscles, higher activity metric values indicate greater energy expenditure (Gleiss et al., 2011). Converting DBA to COL requires species-specific calibration experiments which often employ respirometry – the measurement of expired gases – because the rate of oxygen consumption ($\dot{V}_{O_2}$) is related to aerobic metabolism and allows fine-scale estimation of metabolic rate (Wilson et al., 2020; Withers, 1977). Activity–energetics calibration studies have been conducted in many terrestrial taxa (Halsey et al., 2009), but only a few exist for cetaceans and pinnipeds owing to logistical challenges: Steller sea lions (*Eumetopias jubatus*; Fahlman et al., 2013, 2008), Antarctic fur seals (*Arctocephalus gazella*; Jeanniard-du-Dot et al., 2017a; Skinner et al., 2014), northern elephant seals (*Mirounga angustirostris*; Maresh et al., 2014), Weddell seals (*Leptonychotes weddellii*; Williams et al., 2004), harbor porpoises (*Phocoena phocoena*; Otani et al., 2001) and common bottlenose dolphins (*Tursiops truncatus*; Williams et al., 1993, 2017; Yazdi et al., 1999).

Numerous factors can affect the relationship between activity metrics and energy expenditure, including tag position on the animal, locomotion type, non-movement-based energy expenditure, and experimental/analytical design (for reviews, see Gleiss et al., 2011; Halsey, 2017; Halsey et al., 2009; Wilson et al., 2020). Several studies have found no relationship between activity and energy expenditure in diving animals (Halsey et al., 2011a; Ladds et al., 2017) and some have argued that some correlations may not be as strong as they appear because of the type of metric used (Halsey, 2017; although see Wilson et al., 2020 for a response). However, activity is relatively straightforward to measure in many taxa using biologging devices, and movement may serve as a robust estimate of energy expenditure for some species and under certain circumstances.

To our knowledge, only one other study has attempted to correlate ODBA with energy expenditure in common bottlenose dolphins (John, 2020). Our study sought to determine this correlation with five dolphins of different body sizes. We measured breath-by-breath $\dot{V}_{O_2}$ in trained common bottlenose dolphins across a range of activity levels. The dolphins wore

kinematic tags while swimming subsurface laps. We modeled ODBA–$\dot{V}_{O_2}$ after normalizing by mass. We developed this activity–energetics calibration across a range of body sizes to improve predictions of COL from movement data collected from free-ranging cetaceans and to demonstrate the utility of activity as a proxy for energy use.

MATERIALS AND METHODS
Study site
We studied six male common bottlenose dolphins (*Tursiops truncatus* Montagu 1821) at Dolphin Quest Oahu, a public display zoological facility located on Oahu, Hawaii, accredited by the Alliance of Marine Mammal Parks and Aquariums and certified by American Humane. The dolphins resided in four natural seawater lagoons totaling ∼1420 m^2. The swim trial area was between 1.5 and 3.0 m in depth. Water temperatures during the trials were 25–26°C with an annual range of 24–28°C.

Experimental design and data collection
Swim trial design
Swim trials were conducted in May 2017, 2018 and 2019. Trials were conducted in the morning following an over-night fast, with each animal completing one trial per day. In each trial the tag was placed between the blowhole and dorsal fin. The dolphin remained relaxed at station for ∼1 min before the pneumotachometer was placed over the blowhole. The dolphin breathed into the pneumotachometer for 1.2–10.3 min (median=2.3 min, IQR=2–3.1 min) to measure resting metabolic rate (RMR). The dolphin was then asked to swim to a trainer ∼30 m away and return to station, while remaining below the surface and without stopping (Fig. 1). Twelve trials contained speed data; assuming individuals swam the same distances in trials without speed data, individual mean lap distance (LD) traveled varied between 78 and 86 m owing to variable curvature at the turn around (Table 1). Upon returning to station, the dolphin breathed several times into the pneumotachometer (median=3 breaths, IQR=3–4 breaths), before swimming another lap, and repeating this process for 8–12 total laps before recovery (Fig. 2). Thus, each trial consisted of a pre-swim rest period, 8–12 laps of active swimming (median=10 laps, IQR=9–10 laps), and a recovery period (2.7–9.1 min). The dolphins primarily used consistent stroking, with minimal gliding at the lap mid-point and during the last several seconds before reaching station.

In each trial, animals were asked to swim each lap at approximately the same speed, but were asked to vary speed between trials to obtain inter-trial variation in swim speed. Lap and station durations varied slightly among individuals (Table 1). All breaths were spontaneous – the animals were not cued to breathe. All resting and swim trials were conducted post-absorptive (i.e. no food consumed for >12 h). This protocol was approved by Duke University's Institutional Animal Care & Use Committee (protocol no. A045-17-02).

Respirometry data collection
We measured respiratory flows using a custom-made Fleisch type pneumotachometer (adm+ engineering, Valencia, Spain) equipped with a low-resistance laminar flow matrix (item Z9A887–2, Merriam Process Technologies, Cleveland, OH, USA). A differential pressure transducer (Spirometer Pod, ML 311, ADInstruments, Colorado Springs, CO, USA) was connected to the pneumotachometer with two 310 cm lengths of 2 mm I.D., firm-walled, flexible tubing. The differential pressure transducer was connected to a data acquisition system (Powerlab 8/35, ADInstruments) and the data were captured at 400 Hz and displayed on a laptop computer running LabChart (v. 8.1, ADInstruments). The differential pressure was used to determine
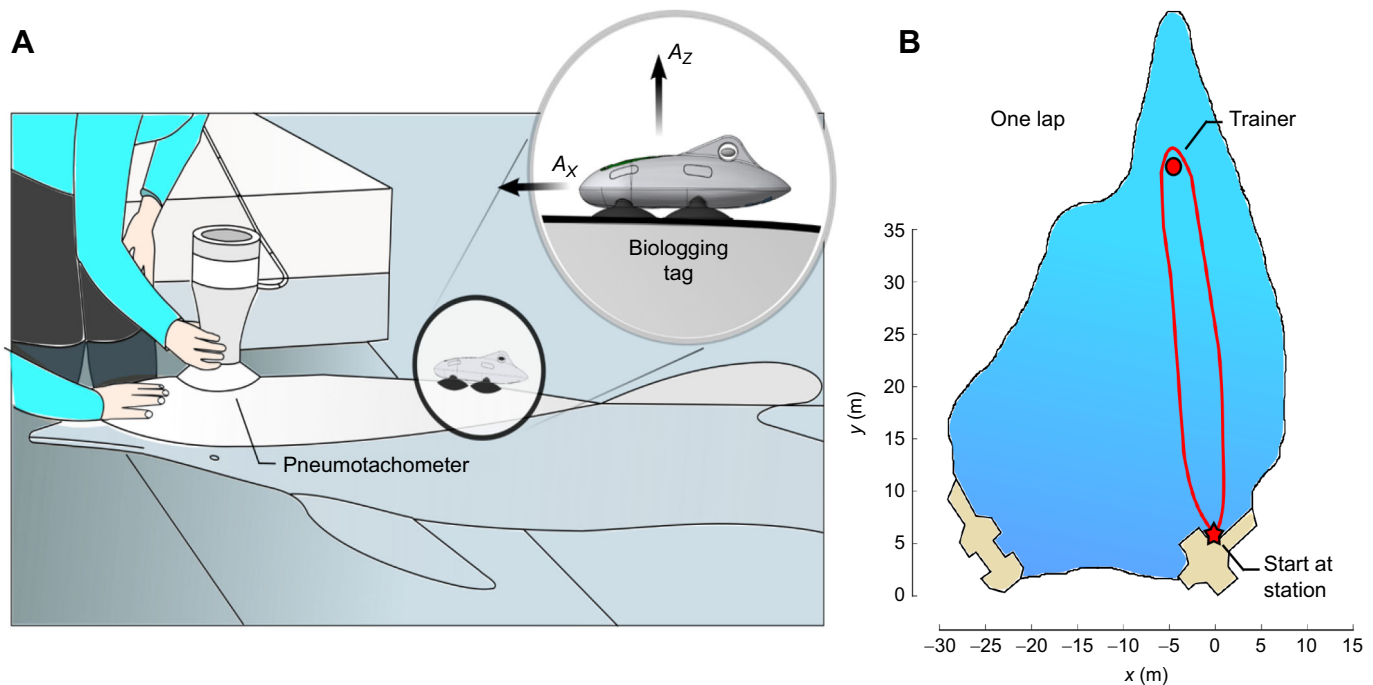
Fig. 1. Experimental setup. (A) Positioning of the pneumotachometer and biologging tag on the animal. The pneumotachometer measured exhalations and inhalations at station (1) during rest before the start of the first lap, (2) after each lap and (3) during a recovery period after the last lap. A_X and A_Z represent acceleration in two of the three axes measured by the accelerometer. (B) Overhead view of experimental pool. The dolphins swam approximately 80 m total distance during each lap.

flow rate and was calibrated using a 7.0 liter calibration syringe (Series 4900, Hans-Rudolph Inc., Shawnee, KS, USA).

Gas concentrations (O_2 and CO_2) were subsampled via a port in the pneumotachometer and passed through a 310 cm length of 2 mm I.D., firm-walled, flexible tubing and a 30 cm length of 1.5 mm I.D. Nafion tubing, to a fast-response O_2 and CO_2 analyzer (Gemini respiratory monitor, CWE Inc., with a 95% response time below 200 ms at a flow rate of 200 ml min^{-1}). The gas analyzer was connected to the data acquisition system and sampled at 400 Hz. The gas analyzer was calibrated before each day's first trial using a commercial mixture of 5% O_2, 5% CO_2 and 90% N_2 (product no. 17 L-340, GASCO, Oldsmar, FL, USA). We used ambient air to check the calibration before and after each trial.

Kinematic data collection
We used three combinations of sensor packages and instrument housings. All contained tri-axial accelerometers, magnetometers, and temperature and pressure sensors. We conducted four trials

using a digital acoustic recording tag (DTAG, version 3; Johnson and Tyack, 2003), 19 trials with an IMU sensor (ActiGraph, Pensacola, FL, USA) and 12 trials with an MTag containing an OpenTag3 sensor (Loggerhead Instruments, Sarasota, FL, USA). Both the IMU and MTag housings closely approximated the shape, profile and attachment mechanism of a DTAG, and both contained gyroscopes in addition to the DTAG sensor types. The MTag also measured speed (Gabaldon et al., 2019).

Body mass data collection
Body mass was measured every 2 weeks using an Altralite scale (Rice Lake Weighing Systems, USA) with a GSE 250SS indicator (GSE Scale Systems, USA; ±0.1 kg).

Data analyses
Respirometry data processing
Methods used to process respirometry data are described in detail in Appendix 1.

Table 1. Morphometrics, respiratory parameters, and experimental trial results for six common bottlenose dolphins

ID	Body mass (kg)	Length (cm)	Age (yr)	RMR (ml O_2 min^{-1})	N	Resting $\dot{V}_{CO_2}$ (ml min^{-1})	S	Lap (s)	Station (s)
83H1	141–146	234	10	583±204	12	513±194	8	24, 22–26	18, 12–31
01L5	149–156	239	23	430±207	13	352±178	9	32, 28–36	20, 16–26
63H4	177	254	27	495±171	4	467±177	NA	NA	NA
9ON6	186–190	249	21	577±262	11[a]	474±212	9	25, 24–26	13, 10–21
6JK5	209–210	259	24	388±222	13[a]	343±182	6	28, 25–31	21, 16–26
9FL3	243–247	274	34[b]	608±410	9	489±344	3	20, 20–21	22, 19–28

Body mass (range of mass in May of different years individual was sampled), age in 2019, resting metabolic rate (RMR) oxygen consumption ($\dot{V}_{O_2}$), number of trials used to calculate resting measurements (N), resting carbon dioxide production ($\dot{V}_{CO_2}$), number of swim trials (S), lap duration (s) median and IQR, and station duration (s) median and IQR. Sample sizes for RMR metrics=N. Sample sizes for lap and station metrics=S.
[a]Each had one trial without CO_2 recorded, resulting in RMR $\dot{V}_{CO_2}$ calculated from 10 and 12 trials, respectively.
[b]Individual 9FL3 was collected from the wild in the 1980s; age is estimated.
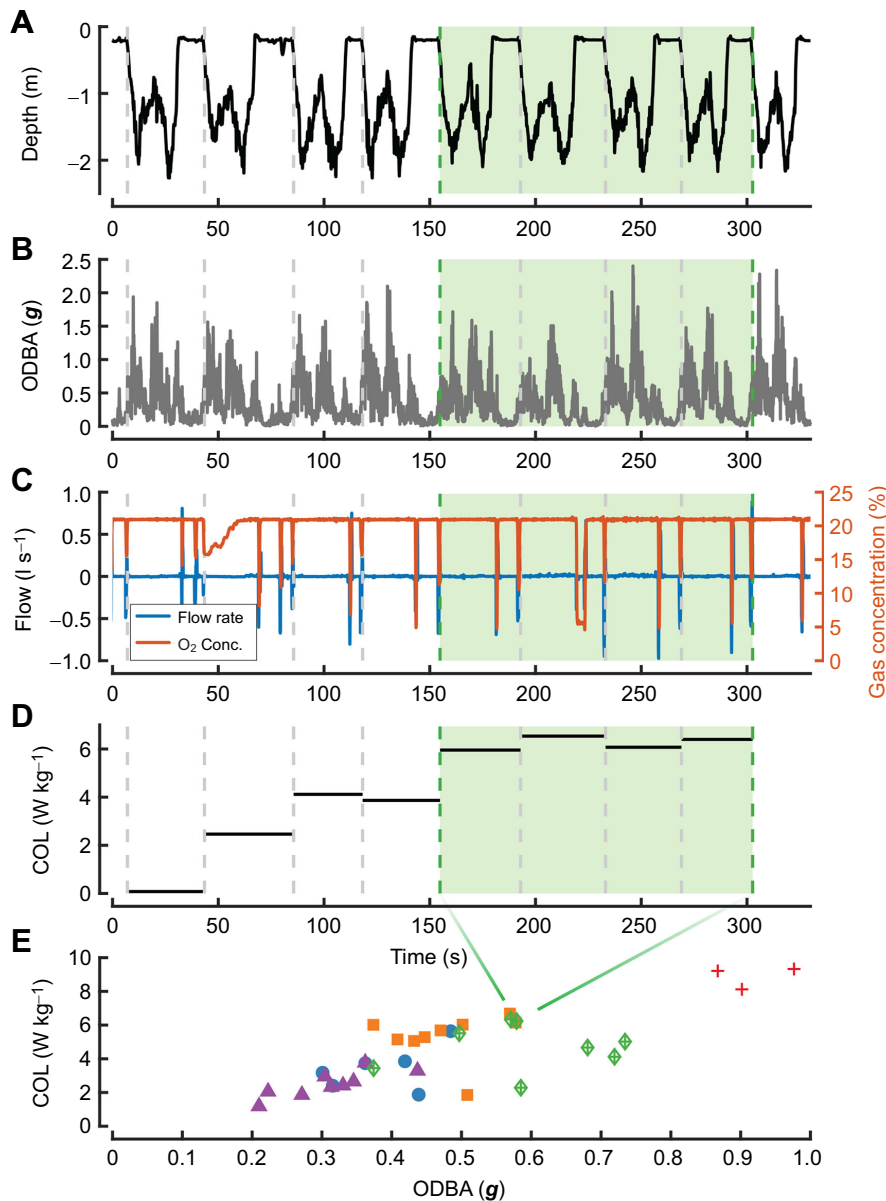
Fig. 2. Experimental data: how the model was derived. A representative 9-lap trial is shown in A–D, from the start of lap 1 to the end of lap 9, with each lap marked by a vertical dashed line. The steady-state $\dot{V}_{O_2}$ period is highlighted in green. (A) During each lap the animal was submerged (depth<0 m) followed by a period at station (depth=~0 m). The depth at the lap midpoint was shallower, seen as the spike near −1 m depth. (B) Larger overall dynamic body acceleration (ODBA) values correspond with swimming during the lap. (C) Respiratory flow, as well as expired O_2 and CO_2 concentration, were measured during breaths after each lap. (D) Although intra-trial ODBA was relatively consistent across laps, cost of locomotion (COL) took several laps to reach steady state. (E) The results from all steady-state swim trials included in the analysis. Green lines point to the trial used in A–D.

Resting metabolic rate

We calculated RMR (ml O_2 min^{-1}) as the $\dot{V}_{O_2}$ during the last 70 s of each pre-swim rest phase of a trial. We chose 70 s because it was the duration of the shortest rest phase of the 62 trials we used for resting calculations (Table 1). We also calculated $\dot{V}_{CO_2}$ over the same duration (Table 1). We predicted basal metabolic rate (BMR) using Kleiber's allometric equation for mature terrestrial mammals (Fahlman et al., 2013; Kleiber, 1975) and divided the observed mean individual RMR (Table 1) by predicted BMR to obtain Kleiber ratios.

Determining steady-state

We performed a segmented linear regression to identify the number of laps required to reach steady-state $\dot{V}_{O_2}$ (Appendix 2). Dolphins usually reached steady-state by lap 4, so we chose the start of lap 5 as the beginning of steady-state for all animals. We made exceptions for four trials in which dolphins missed a breath (i.e. took a breath outside of the pneumotachometer) during lap 5 and, in these trials, steady-state instead began at lap 6. The steady-state period ended at

the beginning of the last lap of each trial, as the O_2 consumed following this lap included recovery of the O_2 debt.
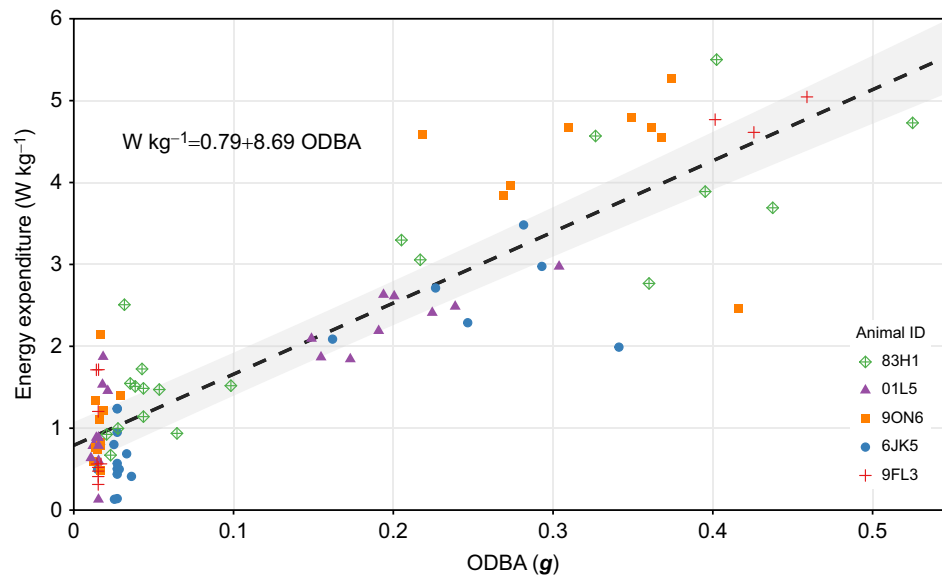
Total energy expenditure

We calculated total energy expenditure by dividing V_{O_2} by the total steady-state duration ($D_{SS,Lap}+D_{SS,Station}$) and converted to W using a conversion factor of 20.1 J ml^{-1} O_2, which assumes the animal is using a representative mixture of carbohydrates, lipids and proteins (Hill et al., 2012; Williams et al., 2017).

Swimming/active metabolic rate and cost of locomotion (COL)

In order to separate RMR from COL, we calculated COL (W) as:

$$\text{COL} = (V_{O_2,SS} - \text{RMR}(D_{SS,Lap} + D_{SS,Station}))D_{SS,Lap}^{-1} 60^{-1} 20.1,$$

(1)

where $V_{O_2,SS}$ is the volume (ml) of O_2 consumed during steady-state, RMR is resting metabolic rate (ml O_2 min^{-1}), $D_{SS,Lap}$ is the duration (min) submerged during steady-state, and $D_{SS,Station}$ is

Fig. 3. Total energy expenditure versus ODBA. Resting and steady-state energy expenditure for five dolphins. Each point below 0.1 ODBA represents the mean resting metabolic rate (RMR) during the last 70 s of the resting duration of a trial, versus the mean ODBA during the rest period (N=58 trials). Each point above 0.1 ODBA represents mean energy expenditure during the steady-state portion of a trial, versus the mean ODBA of the entire steady-state period (lap+station; N=35 trials).

the duration (min) at station (not submerged) during steady-state. The COL was normalized (COL$_{norm}$; W M_b^{-1}) by dividing COL by body mass (M_b; kg) measured within 2 weeks of a trial. We excluded trials from the COL analysis if they contained fewer than 8 laps or if the animal took multiple breaths outside of the pneumotachometer: more than one during steady-state or more than three during the entire trial. For the trials we included in the analysis, missed breaths were replaced with the median breath V_{O_2} of the corresponding trial.

Comparing swimming/active metabolic rate with previous studies
For comparison with Williams et al. (2017), we calculated mass-specific $\dot{V}_{O_2,sCOL}$ (ml O$_2$ kg^{-1} min^{-1}) as:

$$\dot{V}_{O_2,sCOL} = COL\, M_b^{-1} 20.1^{-1} 60. \qquad (2)$$

Tag data processing
We calculated ODBA following Wilson and colleagues (2006), using a running mean of 2 s to filter out static acceleration based on our average fluking rate (1.2 Hz). We calculated per-trial ODBA in two ways. To compare against total energy expenditure, we took the mean ODBA during the rest period before the first lap, and the mean ODBA during each trial's entire steady-state period ($D_{SS,Lap}$+$D_{SS,Station}$). Tag data were unavailable for 19 of the 58 RMR trials included in the total energy expenditure analysis; mean individual ODBA during rest was used in place of measured values for those RMR trials. In the COL analysis, we calculated mean ODBA during only the submerged portion of the steady-state period (the periods at station were excluded), to match the COL calculations (Fig. 2). We processed tag data and calculated pitch using custom-written scripts in MATLAB (v. 2018a), available at soundtags.org. We computed lap distance traveled values from the MTag trials using calibration parameters and estimation methods detailed in Gabaldon et al. (2019).

Power, cost of transport and stroke frequency
We calculated power (W kg^{-1}) using two methods, both using only the 12 trials (five individuals) that used Mtags to record speed. Speed was defined as the distance (m) traveled during steady-state, divided by the time spent swimming during steady-state ($D_{SS,Lap}$). To compare with Yazdi et al. (1999), we divided steady-state V_{O_2} by the entire steady-state duration ($D_{SS,Lap}$+$D_{SS,Station}$), and termed this

method 'average power'. To compare with Williams et al. (1993), we estimated RMR at station by multiplying individual mean RMR by the steady-state station duration ($D_{SS,Station}$), and subtracted this
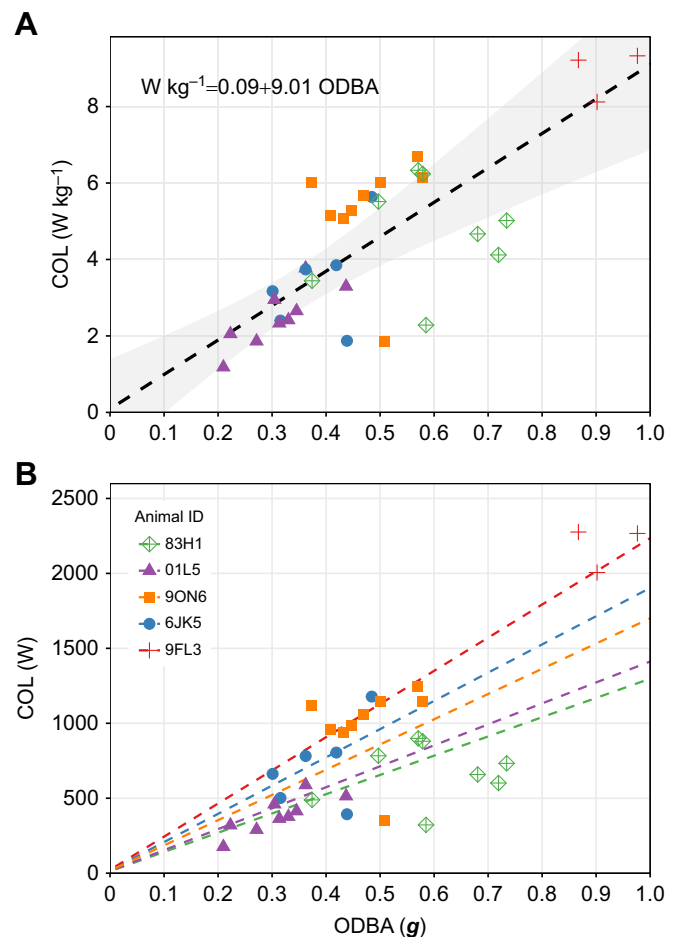
Fig. 4. Predicted cost of locomotion. Each point represents per-trial COL (RMR subtracted). (A) Each COL value is normalized by body mass; the line is the least squares regression, and the shaded area is the ±95% CI. (B) COL is plotted against individual predicted COL (dashed lines) from panel A's regression.

resting station V_{O_2} from steady-state V_{O_2}, before dividing the remainder by duration spent swimming ($D_{SS,Lap}$). We termed this method 'station RMR subtracted'. We fit regressions to both power datasets, as described below.

Total cost of transport (COT; here in J kg^{-1} m^{-1}) is power (W kg^{-1}) divided by speed (m s^{-1}), and is the amount of energy required to move 1 kg of M_b over 1 m (Schmidt-Nielsen, 1995). We divided both power regressions by speed to obtain COT fits, and compared against the 'station RMR subtracted' per-trial power values divided by speed.

To calculate stroke frequency, we used the pitch signal to count fluke strokes and defined stroke frequency as the sum of fluke strokes during steady-state divided by the duration the animal was submerged (i.e. not at station) during steady-state. We compared stroke frequency with $\dot{V}_{O_2}$ calculated as the steady-state V_{O_2} divided by the same steady-state submerged duration, in order to compare with Williams et al. (2017).

Statistics

We performed all statistical analyses in R 4.0.2 (https://www.r-project.org/), except for the intraclass correlation coefficient (ICC) analysis described below. The breakpoint analysis we used to determine the beginning of steady-state $\dot{V}_{O_2}$ is described in Appendix 2.

In the total energy expenditure analysis, we used a linear regression from the nlme package (https://CRAN.R-project.org/package=nlme), with mass-specific energy expenditure (using both RMR and steady-state expenditure; W kg^{-1}) as the response variable and mean ODBA (calculated either during the RMR period or during the entire steady-state period) as the predictor variable, with individual dolphin as a random effect (random intercept only). Mixed-effects models are widely used when interpretations are desired for a population outside of those sampled (individuals in this instance; Ramsey and Schafer, 2013), and 'represent a compromise between assuming no effects and fully independent effects of the levels of a factor' (Kéry, 2010). We performed a likelihood ratio test (LRT) on the fixed effect (ODBA) against a reduced model without ODBA.

For the COL analysis, we used weighted linear regression from the nlme package with COL$_{norm}$ as the response variable, mean ODBA (g) as the predictor variable, and individual dolphin as a random effect (fixed intercept, random slope). A fixed intercept was used because with RMR subtracted, each individual's COL should increase with activity level from a similar starting point (intercept). Random slopes were used to account for potential individual differences in the relationship between COL and activity. We compared this model against a random intercept, fixed slope model in Appendix 3. Mean ODBA squared was included as a fixed variance term [using weights=varFixed($\sim$ODBA^2) inside the lme() function] to account for heteroscedasticity because the residual variance was proportional to ODBA^2. We performed identical LRTs on the COL models as described above.

ICC is a reliability index that reflects both the degree of correlation and agreement between measurements (Koo and Li, 2016). ICC can be used to assess reliability in test–retest situations; in this case, we calculated ICC by comparing each trial's measured COL with each trial's predicted COL using single measures statistics. We used a third-party MATLAB toolbox to facilitate ICC statistics computation (https://www.mathworks.com/matlabcentral/fileexchange/22099-intraclass-correlation-coefficient-icc).
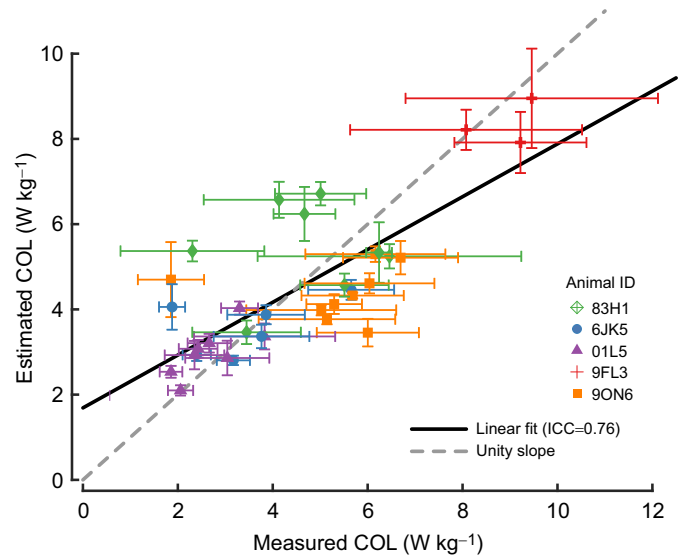
Fig. 5. How well does the model predict COL? Each point represents each trial's measured COL compared with the estimated COL. The horizontal error bars represent steady-state per-lap COL SD as measured from $\dot{V}_{O_2}$, and the vertical error bars represent steady-state per-lap COL SD as estimated from the ODBA–COL correlation.

For the power and COT analyses, we conducted nonlinear least squares regressions using third degree polynomials, with all terms constrained to be positive, as increasing speed should result in increasing energy expenditure. All statistics are means±s.d. unless stated otherwise. All confidence intervals were calculated to estimate the population response [i.e. using 'level=0' inside predict()], though given the mixed-effect framework it is important to note that the uncertainty estimate of the fixed effect (i.e. ODBA) is dependent on the estimates of the random effect variance.

Models were fit with maximum likelihood for LRTs, while reported coefficients, confidence intervals and figures are the restricted maximum likelihood fits. We visually analyzed model residuals to assess assumptions of homoscedasticity, linearity and normality. We used an alpha level of 0.05 for all statistical tests.

RESULTS
Resting metabolic rate
Post-absorptive resting $\dot{V}_{O_2}$ (N=62 trials) and $\dot{V}_{CO_2}$ (N=60 trials) varied among individuals (Table 1). The median individual Kleiber ratio was 0.99 (range=0.71–1.42).

Total energy expenditure
Thirty-five swim trials were included in the steady-state breakpoint, total energy expenditure and COL analyses (representing five individuals; S, Table 1). Ten of the 35 trials had 1–3 breaths replaced before the analyses: in 6 trials the missed breath(s) occurred before steady-state; 4 trials had one missed breath during steady state. In these 4 trials, replacing the missed breath by the trial's median breath V_{O_2} increased the steady-state $\dot{V}_{O_2}$ by 1.2–7.4%. Replacing the missed breath by the trial's maximum breath V_{O_2} would have increased the steady-state $\dot{V}_{O_2}$ by 13.5–23.9%.

There was a significant (LRT=157.6, P<0.0001), positive, linear relationship between energy expenditure and ODBA (intercept=0.79, 95% CI=0.51–1.07, t=5.56; slope=8.69, 95% CI=7.83–9.55, t=20.07; d.f.=87; N=93 trials: 58 rest periods and 35 steady-state periods; Fig. 3).
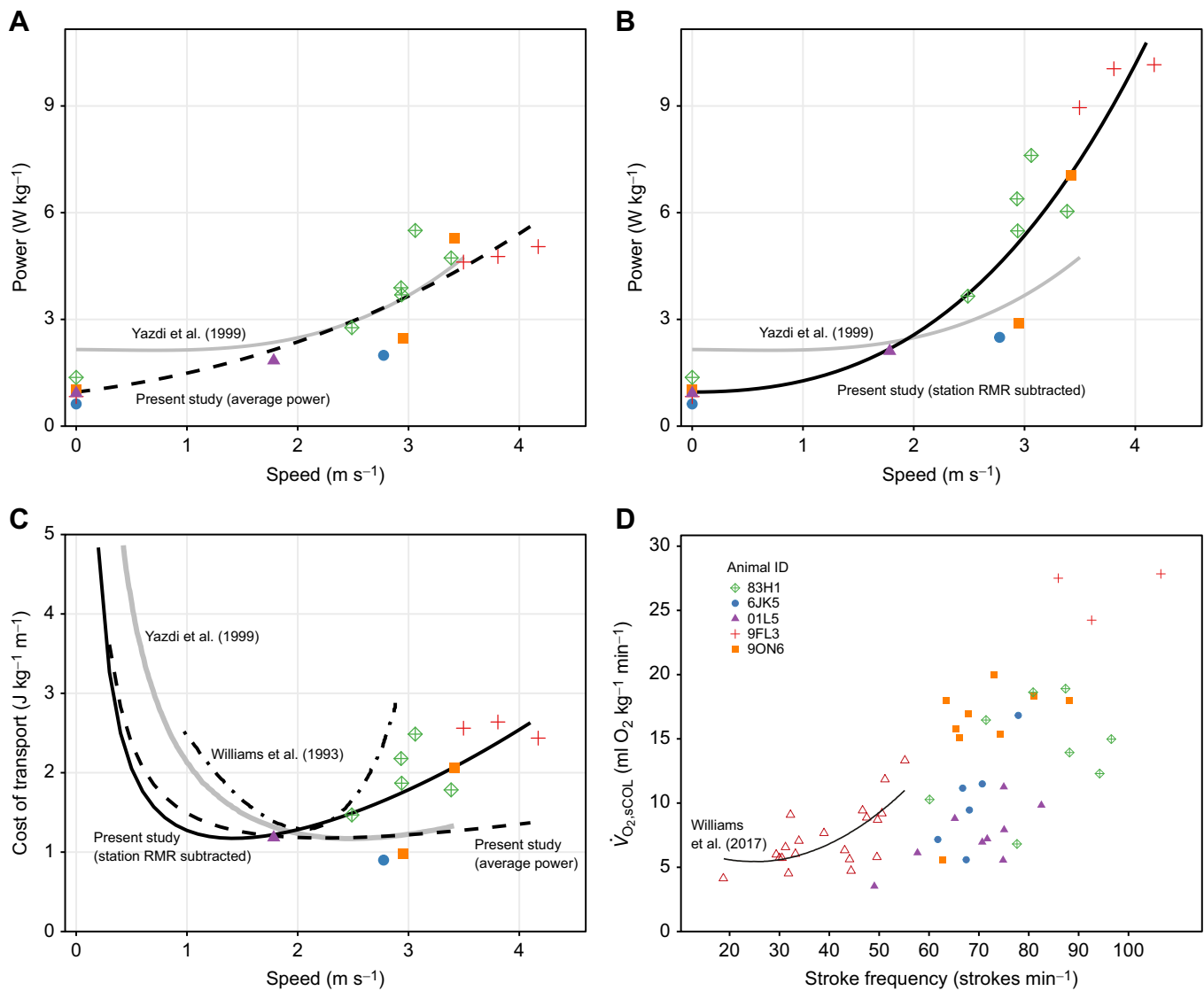
Fig. 6. Power, cost of transport and stroke frequency. Points in A–C at speeds above 0 m s^{-1} represent the 12 trials where the Mtags were used to measure speed. (A) Points at speed 0 m s^{-1} represent individual mean RMR for the 5 dolphins in the current study. Points above speed 0 m s^{-1} are calculated using the 'average power' method. The dashed line is the regression fit for the present study; the gray line is the fit from Yazdi et al. (1999). (B) Points above speed 0 m s^{-1} are calculated using the 'station RMR subtracted' method. The solid line is the regression fit for this study; the gray line is the fit from Yazdi et al. (1999). (C) Cost of transport. Points represent the points in B divided by speed. The fits represent the fits in A and B divided by speed, in addition to the COT fit from Williams et al. (1993). (D) Red open triangles are combined per dive $\dot{V}_{O_2}$ for four dolphins in Williams et al. (2017); the line is the least-squares regression from the same study. Other symbols are per-trial stroke-matched $\dot{V}_{O_2,sCOL}$ from the present study for comparison.

Cost of locomotion (COL)

There was a significant (LRT=14.9, P=0.0001), positive, linear relationship between COL$_{norm}$ and ODBA (intercept=0.09, 95% CI=−1.24–1.42, t=0.14; slope=9.01, 95% CI=5.61–12.40, t=5.42; d.f.=29; N=35 trials; Fig. 4A).

Predicted COL were compared with measured values (Fig. 4B, Fig. A3). The results from the ICC analysis indicate that the COL model fit overestimates COL at lower effort levels and underestimates COL at higher effort levels compared with the measured values (Fig. 5). The one-way random, single measures ICC was 0.76 (95% CI=0.58–0.87, P=2.7×10^{-8}), indicating moderate to good agreement between measured and predicted COL (Koo and Li, 2016). The fit is also visualized using Bland–Altman plots in Appendix 3 (Fig. A3C).

Power, cost of transport, and stroke frequency

'Average power' was modeled as power (W kg^{-1})=0.010v^3+0.144v^2+0.378v+R (N=17, d.f.=14, s.e. of the regression=0.77; Fig. 6A), where v is swimming speed (m s^{-1}) and R is mean RMR (0.958±0.276 W kg^{-1}). 'Station RMR subtracted' power was modeled as power (W kg^{-1})=0.087v^3+0.228v^2+0v+R (N=17, d.f.=14, s.e. of the regression=1.22; Fig. 6B), where v and R are the same as above.

Minimum COT (J kg^{-1} min^{-1}) was similar between the 'average power' method (1.18 J kg^{-1} min^{-1}; 2.3 m s^{-1}) and the 'station RMR subtracted' method (1.17 J kg^{-1} min^{-1}; 1.4 m s^{-1}), although speed at minimum COT differed (Fig. 6C).

Per-trial COL versus mean stroke frequency (range=49–106 strokes min^{-1}) was compared with values from Williams

et al. (2017); overall, there was a positive, non-linear relationship between $\dot{V}_{O_2,sCOL}$ and stroke frequency when the two studies were combined (Fig. 6D).

DISCUSSION

Here, we show that ODBA and COL are correlated during experimental, aerobic, subsurface swim trials with common bottlenose dolphins. The strength of the correlation between ODBA and COL varied among individuals, so predictions regarding individual dolphins should be interpreted cautiously. This is perhaps unsurprising, given the limited number of trials for each individual. However, there was a significant linear relationship between ODBA and energy expenditure when all individuals were considered together (Figs 3 and 4A). Some other studies have been unable to find a relationship between DBA and COL. Below, we discuss factors that may confound the relationship between DBA and COL and discuss the implications of enhanced COL estimates.

Limitations

Some individuals reached higher steady-state activity levels than others (Fig. 4), which is not unexpected given individual differences in fitness and swimming efficiencies related to morphometrics. Individual predictions largely tracked individual measurements (Fig. 4B). One individual (9ON6) had higher than predicted COL values (Fig. 4), suggesting that some individual differences may remain, even after accounting for variation in M_b. All dolphins remained submerged while swimming, but it is likely that some individuals may have incurred variable wave drag if they swam close to the surface during parts of the trial. Wave drag occurs when swimmers are within three body diameters of the surface or bottom (Fish, 1993a; Hertel, 1969). Although DBA metrics should account for the effect of wave drag, acceleration and $\dot{V}_{O_2}$ should increase with increased drag as the animal compensates with greater effort. Mechanical modeling would help further determine the relative impact of wave drag on activity–energetics correlations.

Tag stability, tag placement and gait changes can affect the DBA–$\dot{V}_{O_2}$ relationship (Gleiss et al., 2011; Wilson et al., 2020). We expect these effects to be minimal in the present study: tag placement was consistent among trials and close to the center of gravity, suction cups kept the tags firmly attached, and the dolphins used consistent stroking.

The mass-specific steady-state $\dot{V}_{O_2}$ (5.5–16.4 ml O_2 kg^{-1} min^{-1}), calculated as in a previous study to estimate the lactate threshold in dolphins (20–29 ml O_2 kg^{-1} min^{-1}; Williams et al., 1993), suggests that the exercise in the present study was primarily aerobic (i.e. submaximal) and therefore a valid measure of aerobic energy expenditure (Wasserman et al., 1967).

Resting metabolic rate

To allow comparisons of energy requirements across species, Kleiber (1975) defined a set of criteria for measurements of BMR: adult animals should be in a non-reproductive state, at rest, post-absorptive and thermoneutral. Many early measurements of marine mammals did not conform to these criteria. As a result, it has been suggested that marine mammals, in general, have resting metabolisms higher than those of terrestrial mammals. More recent studies suggest that BMR across marine mammals may be closer to values in terrestrial taxa, especially considering the sampling bias toward smaller, more active marine mammal species (for a review, see Maresh, 2014). BMR criteria were developed in terrestrial animals, and many marine

mammal studies use the term 'resting' metabolic rate rather than 'basal', to acknowledge the challenges in applying these criteria to marine mammals (Maresh, 2014).

We believe that the RMR measurements in the present study met BMR criteria, including thermoneutrality (Williams et al., 2001). Among studies that met BMR criteria, our RMR values (1.9–4.1 ml O_2 kg^{-1} min^{-1}; calculated from Table 1) were consistent with those from some previous studies (2.7–5.0 ml O_2 kg^{-1} min^{-1}; Noren et al., 2013; Pedersen et al., 2020; van der Hoop et al., 2014; Yeates and Houser, 2008), and lower than others (6.4–7.4 ml O_2 kg^{-1} min^{-1}; Williams et al., 1993; Williams et al., 2001; Williams et al., 2017). Even when the criteria for measuring BMR are met, other factors can influence mass-specific RMR estimates, including body condition, the duration of measurement of RMR, and the animal's familiarity and comfort with the experimental protocol (Fahlman et al., 2018). Individual Kleiber ratios in the present study suggest that BMR in bottlenose dolphins, at least in some studies, may be closer to that of terrestrial mammals than previously thought.

Dynamic body acceleration predicts cost of locomotion

Energy expenditure increased linearly with ODBA, both when measuring total energy expenditure (Fig. 3) and after subtracting RMR to isolate COL (Fig. 4). Past studies have shown that both swim speed and stroke frequency increase exponentially with COL (Fig. 6D) as the effect of hydrodynamic drag increases with increasing speed (Williams et al., 1993). However, regarding the relationship between ODBA and metabolic work, Gleiss et al. (2011) note that 'if ODBA scales linearly with mechanical work, the resultant relationship should be linear, given that mechanical work equals metabolic work (above RMR)'. A linear relationship has been found between DBA and metabolic work in all species tested so far (Wilson et al., 2020), including fish (Wright et al., 2014), pinnipeds (Fahlman et al., 2008), shellfish (Robson et al., 2012), amphibians (Halsey and White, 2010), reptiles (Halsey et al., 2011b), and many terrestrial mammals and birds (Halsey et al., 2009).

Previous marine mammal studies have reported conflicting results; some agree with our finding of a correlation between ODBA and $\dot{V}_{O_2}$ (i.e. a DBA–COL relationship), while others failed to detect a correlation. For example, Ladds et al. (2017) found no relationship between DBA or stroke frequency and $\dot{V}_{O_2}$ in fur seals or Steller sea lions. This could have been caused by thermal substitution, in which the confounding effect of thermal heat loss in cold water interferes with the relationship (Wilson et al., 2020). In our study, animals were housed in a thermoneutral environment (Williams et al., 2001). This may, in part, explain why our results showed a correlation, and why studies investigating homeotherms that operate both in air and cold water need to account for thermal substitution (Wilson et al., 2020).

It is important to note that activity–energetics correlations which use two cumulative metrics can produce a strong correlation between uncorrelated variables because time is on both axes – termed the 'time trap' (Halsey, 2017; Ladds et al., 2017). It has been argued that some activity–energetics correlations appear stronger than they are owing to using two cumulative metrics. This does not necessarily invalidate a correlation, but it is best to use at least one mean value (Wilson et al., 2020). In the present study we used two mean values to avoid this issue: mean ODBA and $\dot{V}_{O_2}$.

Swim speed, power, cost of transport and stroke frequency

The dolphins' mean lap speeds (2.3–4.2 m s^{-1}) were similar to the observed swim speeds of bottlenose dolphins in both human

care (1.2–6.0 m s^{-1}; Fish, 1993b) and in the wild (1.6–5.6 m s^{-1}; Rohr et al., 2002). Our power and COT values were lower at slower swim speeds than other studies owing to the lower RMR values in the present study (Fig. 6A–C). Our 'average power' method closely matched Yazdi et al. (1999) at speeds over 2 m s^{-1} owing to their similar calculation (Fig. 6A). However, we feel that the' station RMR subtracted' method (Fig. 6B) more closely approximates the true relationship between power and speed by accounting (i.e. subtracting) for rest periods in between swimming periods. The 'station RMR subtracted' minimum COT (1.17 J kg^{-1} min^{-1}) was close to the minimum identified by Williams et al. (1993; 1.29 J kg^{-1} min^{-1}) but at a slower speed (1.4 m s^{-1}) than that of Williams et al. (1993; 2.1 m s^{-1}). The 'station RMR subtracted' COT fit is also higher than the fit of Yazdi et al. (1999) and lower than the fit of Williams et al. (1993) at speeds over 2 m s^{-1} (Fig. 6C).

The mass-specific $\dot{V}_{O_2,sCOL}$–stroke frequency correlation in the present study was similar to that reported in a previous study (Williams et al., 2017), despite differences in experimental design (Fig. 6D). Both $\dot{V}_{O_2}$ and stroke frequency were higher in the present study, extending the range of our knowledge of the relationship between $\dot{V}_{O_2}$ and stroke frequency.

### Implications and future directions

Estimates of COL are necessary to address fundamental ecological questions associated with foraging, migration and other life history events (Goldbogen et al., 2019; Williams et al., 2020). Such estimates are also needed to measure the impacts of sublethal threats to marine mammals (Williams et al., 2017). Several efforts are currently underway to determine whether anthropogenic disturbance of marine mammals can have population-level fitness consequences. Estimates of the increased metabolic cost of a response (e.g. swimming rapidly away from a perceived threat) are required to parameterize PCoD models. In the most acute cases, anthropogenic sounds may result in changes in physiology and behavior that cause direct or indirect trauma (Fahlman et al., 2021), but sub-acute changes in behavior and physiology may result in cumulative long-term consequences for fitness. For example, under the predation risk framework, an animal may perceive a human-caused disturbance as a predator and modify their physiology or behavior to reduce predation risk (Frid and Dill, 2002). Scaling the responses of individuals to population-level impacts requires measuring a response and integrating the response with the population's physiology, energetics and life history (King et al., 2015; Nabe-Nielsen et al., 2018; Nowacek et al., 2016; Schwacke et al., 2017; Williams et al., 2016). Owing to knowledge gaps, few PCoD models have explicitly incorporated the physiological consequences of disturbance, including COL (Pirotta et al., 2018).

Dolphins use a variety of swimming gaits that incorporate different proportions of stroking and gliding to maximize efficiency (Skrovan et al., 1999). The energetic cost of a stroke and of a dive has been shown to be influenced by gait changes (Williams et al., 2017). Future studies should examine the predictive power of different calibration studies on longer duration deployments that include different gaits and dive depths. Similarly, ODBA–$\dot{V}_{O_2}$ predictions from this study should only be applied to free-ranging cetaceans in which the tag is in a similar position and has not slid over the body. Future studies should compare the present study's COL prediction with stroke-based predictions at longer time scales to validate their ability to determine daily energy expenditure. COL estimates will need to be combined with RMR and specific

dynamic action estimates to estimate daily FMR. This could be compared with other daily FMR estimates from ingested calories and labeled isotopes.

Conclusions

Although the strength of the correlation between ODBA and energy expenditure varied among individuals, overall, ODBA and energy expenditure are linearly correlated in common bottlenose dolphins, both when examining total energy expenditure and when isolating the COL. Activity–energetics proxies will benefit from including biomechanical modeling that incorporates drag effects and further refines differences owing to morphometrics and locomotory mode. Further studies are underway to test the ODBA–COL proxy in the present study, and stroke frequency–COL proxies from other studies, on longer duration deployments to quantify their ability to predict daily costs. The approach demonstrated here shows that ODBA may be a useful proxy for the energetic cost of physical activity in bottlenose dolphins; our goal is to apply these techniques to understand locomotion costs in free-ranging cetaceans.
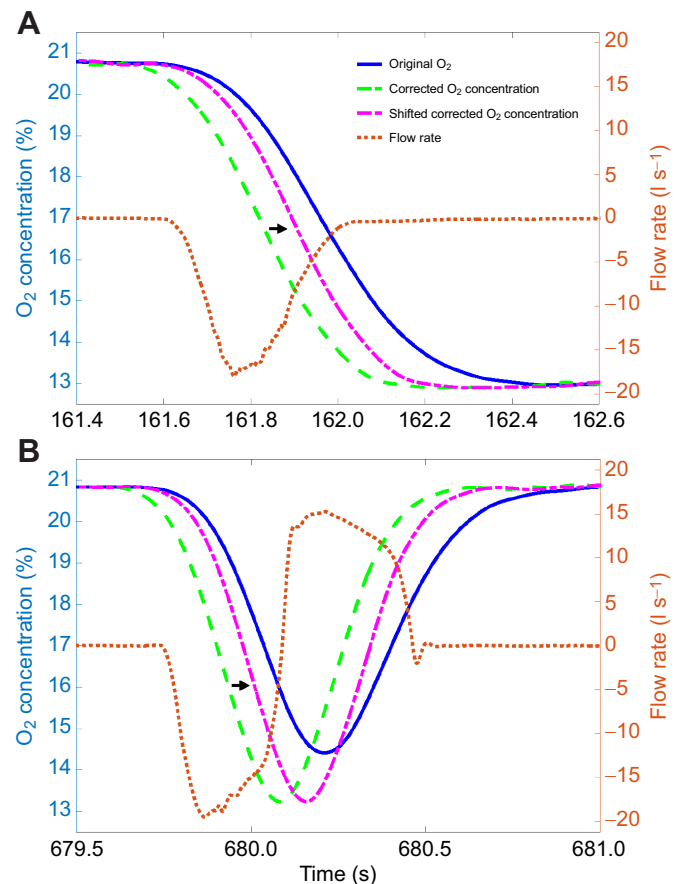
Fig. A1. O$_2$ and CO$_2$ signal correction. Gas concentration signal correction. Here, the O$_2$ correction is displayed; the same correction and tau values were applied to the CO$_2$ signals. (A) During isolated exhalations, the end tidal gas concentration can be assumed. Here, the measured O$_2$ signal (original) was aligned with the flow rate. The end tidal O$_2$ concentration was used to correct the measured O$_2$ signal with an exponential method to obtain the corrected signal. The corrected signal was then shifted to align with the flow rate. (B) The exponential parameters used during the exhale only breaths were then used on typical breaths (exhale immediately followed by an inhale) to correct the measured O$_2$ signal.

APPENDIX 1
Details of the gas concentration processing

In fast-breathing animals, the tubing and gas analyzer response time cause a distortion of the shape, as well as a delay, in the measured signal. We corrected the distortion of both gas concentration signals using a two-exponent equation (Arieli and Van Liew, 1981; Bates et al., 1983; Farmery and Hahn, 2000):

$$C_2 = C_0 + (Y_1 + Y_2) \times \frac{dC_0}{dt} + (Y_1 \times Y_2) \times \frac{d^2C_0}{dt^2}, \quad (A1)$$

where C_2 is the corrected signal, C_0 is the low-pass filtered (5 Hz cut-off) original signal, Y_1 and Y_2 are constants, $\frac{dC_0}{dt}$ is the first derivative of C_0 and $\frac{d^2C_0}{dt^2}$ is the second derivative of C_0. Because most breaths consist of an exhale immediately followed by an inhale, we examined a subset of breaths where the exhalation and inhalation were separated by more than 1 s. We used the return to ambient gas concentration after the exhale in this subset of breaths, as well as the synoptic flow rate, to estimate the true shape of the gas concentration signal (Fig. A1). We varied Y_1 and Y_2 to obtain C_2 in Eqn A1. We found that $Y_1=0.07$ and $Y_2=0.08$ yielded appropriate C_2 values for both O_2 and CO_2 in this subset of exhales and inhales. Using $Y_1=0.07$ and $Y_2=0.08$ in Eqn A1 on typical breaths, O_2 C_2 increased by a median of 18% (IQR 15–23%) compared with O_2 C_0, and CO_2 C_2 increased by a median of 19% (IQR=15–24%) compared

with CO_2 C_0. We used these corrected gas concentrations for all analyses.

To account for the delay caused by the time it takes the subsampled air to travel through the tubing and reach the gas analyzer, we shifted both gas signals to align with the flow rate (Arieli and Van Liew, 1981; Fahlman et al., 2015). We converted all gas volumes to standard temperature and pressure for dry air (STPD; Quanjer et al., 1993). We multiplied the expiratory flow rate by the expired O_2 and CO_2 to calculate $\dot{V}_{O_2}$ and CO_2 production rate ($\dot{V}_{CO_2}$), before integrating $\dot{V}_{O_2}$ and $\dot{V}_{CO_2}$ over each breath to yield the volume of O_2 consumed (V_{O_2}) or CO_2 (V_{CO_2}) produced during each breath (Fahlman et al., 2015). Additionally, the respiratory exchange ratio (V_{CO_2}/V_{O_2}) at rest and during the swim trials is reported in Fig. S1.

APPENDIX 2
Steady-state breakpoint analysis

To determine the beginning of steady-state $\dot{V}_{O_2}$, we used segmented linear regression, with lap number as the predictor variable, and $\dot{V}_{O_2,average}$ as the response variable (segmented package; Muggeo, 2003). A separate model was run per individual. We defined $\dot{V}_{O_2,average}$ by the following equation:

$$\dot{V}_{O_2,average} = V_{O_2,lap}/(D_{lap} + D_{station}), \quad (A2)$$

where $V_{O_2,lap}$ is the volume (ml) of O_2 consumed during station after a lap, D_{lap} is the duration (min) of the lap (when submerged) and $D_{station}$ is the duration (min) at station (not submerged) after
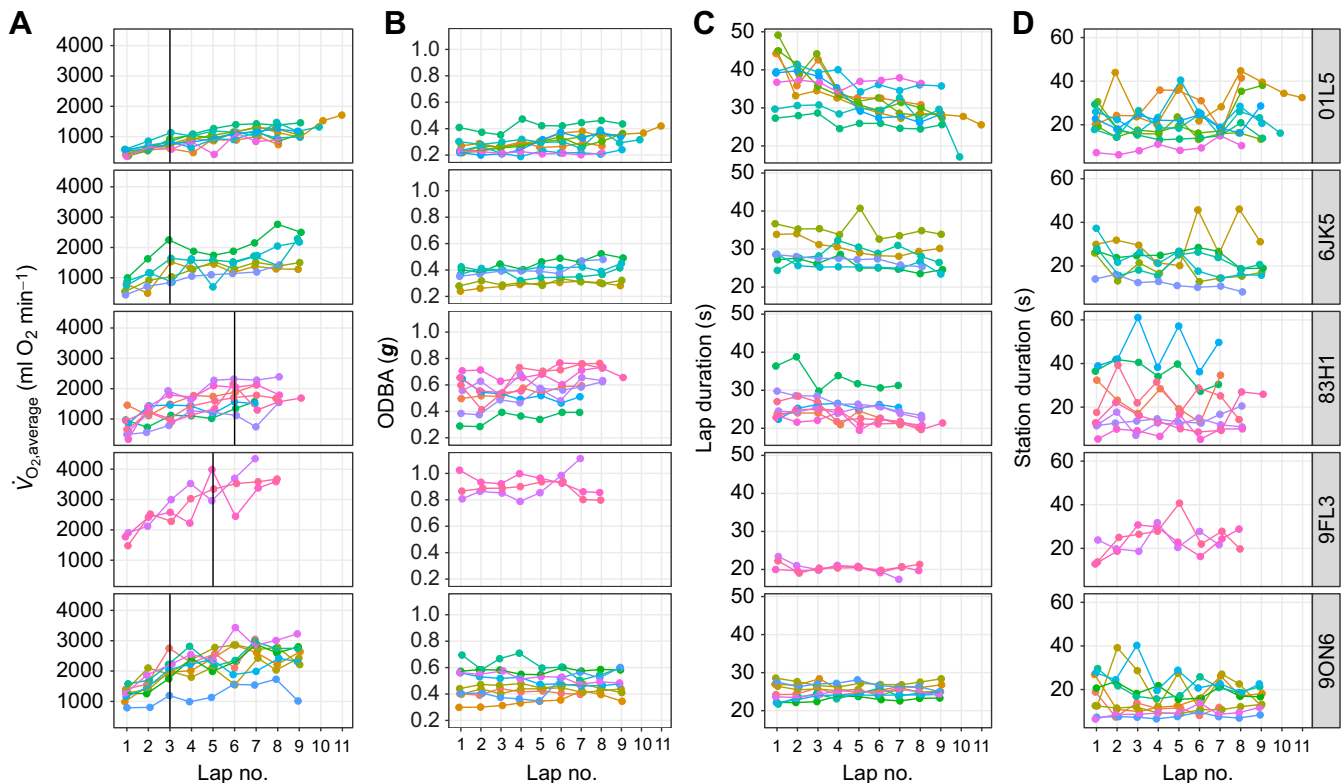
Fig. A2. Steady-state breakpoint analysis and per lap/station metrics. The last lap was removed prior to all analyses, and each line represents one swim trial (N=35). (A) Per-lap $\dot{V}_{O_2}$, calculated as the V_{O_2} measured during station after a given lap, divided by the combined lap and station duration. Vertical lines denote the lap breakpoint identified through per individual segmented regression analysis. (B) Mean ODBA during the lap (excludes ODBA at station). (C) Time spent swimming, calculated from the start of a lap until the animal returned to station. (D) Time at station after a given lap, calculated from the return to station after a given lap, until the animal left for the next lap.

swimming the lap. Some individuals had significant breakpoints while others did not: lap 3 for 01L5 (P<0.047), 6JK5 (P<0.122) and 9ON6 (P<0.002); lap 5 for 9FL3 (P<0.065); and lap 6 for 83H1 (P<0.023).

Fig. A2 demonstrates that even with mean ODBA remaining relatively stable within a trial (Fig. A2B), there was a ramp up in energy expenditure (Fig. A2A), demonstrating that it took several laps to reach steady-state energy expenditure. Lap duration (Fig. A2C) and station duration (Fig. A2D) remained relatively consistent within a trial. We expected between trials to vary in ODBA and lap duration, owing to asking animals for different activity levels between trials.
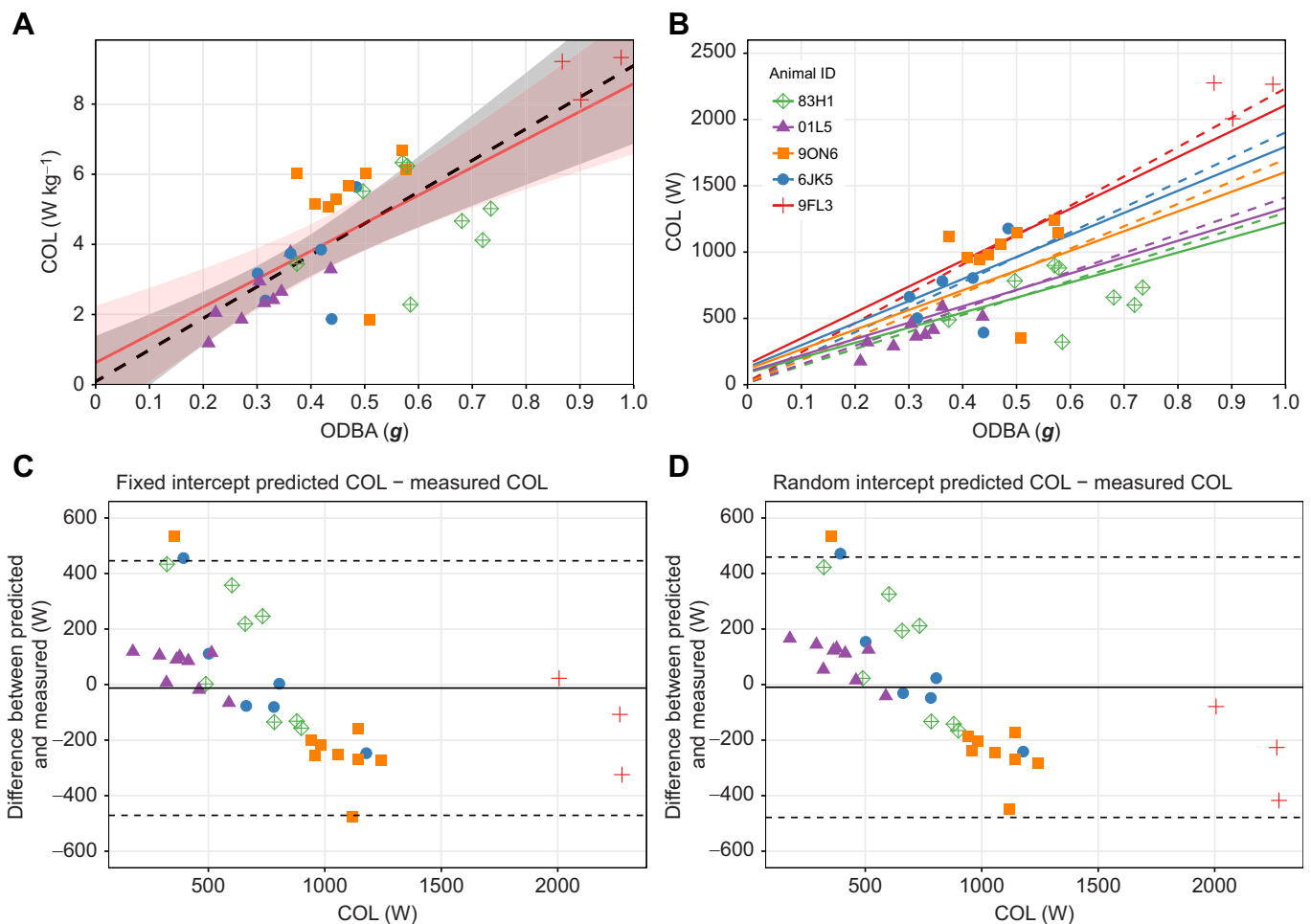
APPENDIX 3
Comparing model fits for ODBA versus normalized COL

Although we believe that the fixed intercept, random slope model (Fig. 4A) is the best approach, we also performed a random intercept, fixed slope model, with all other model parameters staying the same. Just as in the fixed intercept model, there was a significant (LRT=15.8, P=0.0001), positive, linear relationship between COL_{norm} and ODBA (intercept=0.62, 95%

CI=−1.03–2.29, t=0.77; slope=7.95, 95% CI=4.59–11.32, t=4.84; d.f.=29; N=35 trials; Fig. A3A).

Fig. A3A,B demonstrates that the random intercept model predicts greater COL at lower ODBA values than the fixed intercept model, and predicts lower COL at higher ODBA values. We performed Bland–Altman graphical procedures to examine agreement and evaluate the presence of proportional systemic bias; limits of agreement were calculated as the mean difference between predicted and measured COL±1.96×SD of the differences (Bland and Altman, 1986). For each pairwise comparison, we plotted the residuals between the predicted and measured COL. Because most trials fall in the middle of the ODBA range, the Bland–Altman plots (Fig. A3C,D) show little difference between predicted and measured COL between the two models. Potentially, the fixed intercept model better predicts individual 9FL3's COL (Fig. A3D) than in the random intercept model (Fig. A3C). Given the minimal difference between the models, we believe the fixed intercept, random slope model is the better choice; RMR was subtracted from steady-state energy expenditure to obtain COL values, thus each individual's COL should increase from a similar intercept (near zero COL at zero ODBA).

Fig. A3. Comparing COL models. (A) Points are mass-specific per-trial steady-state COL. Dashed line is the fixed intercept, random slope model from Fig. 4A; gray area is 95% CI. The solid line is the random intercept, fixed slope model described in Appendix 3; red area is 95% CI. (B) Points are per-trial steady-state COL. Dashed lines are individual predictions of the fixed intercept, random slope model. Solid lines are individual predictions of the random intercept, fixed slope model. (C) Bland–Altman plot of residuals between fixed intercept, random slope predicted COL and measured COL. Solid line is the mean difference, dashed lines are 95% limits of agreement. (D) Bland–Altman plot of residuals between random intercept, fixed slope predicted COL and measured COL. Lines are the same as in C.

Author contributions
Conceptualization: A.S.A., A.J.R., K.A.S., A.F.; Methodology: A.S.A., A.J.R., K.A.S., J.G., A.M.B., J.R., A.F.; Software: A.S.A., K.A.S., J.G., A.M.B., A.F.; Formal analysis: A.S.A., K.A.S., J.G., A.M.B., A.F.; Investigation: A.S.A., K.A.S., J.G., A.M.B., J.R., A.F.; Resources: A.S.A., A.J.R., K.A.S., J.R., A.F.; Data curation: A.S.A., K.A.S., J.G., J.R., A.F.; Writing - original draft: A.S.A., A.F.; Writing - review & editing: A.S.A., A.J.R., K.A.S., J.G., A.M.B., J.R., A.F.; Visualization: A.S.A., K.A.S., J.G.; Supervision: A.S.A., A.J.R., K.A.S., J.R., A.F.; Project administration: A.S.A., A.J.R., K.A.S., J.G., A.M.B., J.R., A.F.; Funding acquisition: A.S.A., A.J.R., K.A.S., A.F.

Data availability
Data are available from the Dryad Digital Repository (Allen et al., 2022): https://doi.org/10.5061/dryad.6q573n60x.

References
Allen, A. S., Read, A. J., Shorter, K. A., Gabaldon, J., Blawas, A. M., Rocho-Levine, J. and Fahlman, A. (2022). Data from: Dynamic body acceleration as a proxy to predict the cost of locomotion in bottlenose dolphins. *Dryad Dataset.* doi:10.5061/dryad.6q573n60x

Arieli, R. and Van Liew, H. D. (1981). Corrections for the response time and delay of mass spectrometers. *J. Appl. Physiol. Respir. Environ. Exerc. Physiol.* **51**, 1417-1422. doi:10.1152/jappl.1981.51.6.1417

Bates, J. H., Prisk, G. K., Tanner, T. E. and McKinnon, A. E. (1983). Correcting for the dynamic response of a respiratory mass spectrometer. *J. Appl. Physiol. Respir. Environ. Exerc. Physiol.* **55**, 1015-1022. doi:10.1152/jappl.1983.55.3.1015

Bland, J. M. and Altman, D. G. (1986). Statistical methods for assessing agreement between two methods of clinical measurement. *Lancet* **327**, 307-310. doi:10.1016/S0140-6736(86)90837-8

Butler, P. J., Green, J. A., Boyd, I. L. and Speakman, J. R. (2004). Measuring metabolic rate in the field: the pros and cons of the doubly labelled water and heart rate methods. *Funct. Ecol.* **18**, 168-183. doi:10.1111/j.0269-8463.2004.00821.x

Costa, D. P., Worthy, G. A., Wells, R. S., Read, A. J., Waples, D. and Scott, M. D. (2013). Patterns of seasonal metabolic rate variation for bottlenose dolphins in Sarasota Bay, Florida. In 20th Biennial Conference on the Biology of Marine Mammals, p. 49. Dunedin, New Zealand.

Fahlman, A., Wilson, R., Svärd, C., Rosen, D. A. S. and Trites, A. W. (2008). Activity and diving metabolism correlate in Steller sea lion *Eumetopias jubatus*. *Aquat. Biol.* **2**, 75-84. doi:10.3354/ab00039

Fahlman, A., Svärd, C., Rosen, D. A. S., Wilson, R. P. and Trites, A. W. (2013). Activity as a proxy to estimate metabolic rate and to partition the metabolic cost of diving vs. breathing in pre- and post-fasted Steller sea lions. *Aquat. Biol.* **18**, 175-184. doi:10.3354/ab00500

Fahlman, A., Loring, S. H., Levine, G., Rocho-Levine, J., Austin, T. and Brodsky, M. (2015). Lung mechanics and pulmonary function testing in cetaceans. *J. Exp. Biol.* **218**, 2030-2038. doi:10.1242/jeb.119149

Fahlman, A., van der Hoop, J., Moore, M. J., Levine, G., Rocho-Levine, J. and Brodsky, M. (2016). Estimating energetics in cetaceans from respiratory frequency: why we need to understand physiology. *Biol. Open* **5**, 436-442. doi:10.1242/bio.017251

Fahlman, A., Brodsky, M., Wells, R., McHugh, K., Allen, J., Barleycorn, A., Sweeney, J. C., Fauquier, D. and Moore, M. (2018). Field energetics and lung function in wild bottlenose dolphins, *Tursiops truncatus*, in Sarasota Bay Florida. *R. Soc. Open Sci.* **5**, 171280. doi:10.1098/rsos.171280

Fahlman, A., Cozzi, B., Manley, M., Jabas, S., Malik, M., Blawas, A. and Janik, V. M. (2020). Conditioned variation in heart rate during static breath-holds in the bottlenose dolphin (*Tursiops truncatus*). *Front. Physiol.* **11**, 1509. doi:10.3389/fphys.2020.604018

Fahlman, A., Moore, M. J. and Wells, R. S. (2021). How do marine mammals manage and usually avoid gas emboli formation and gas embolic pathology? Critical clues from studies of wild dolphins. *Front. Mar. Sci.* **8**, 25. doi:10.3389/fmars.2021.598633

Farmery, A. D. and Hahn, C. E. W. (2000). Response-time enhancement of a clinical gas analyzer facilitates measurement of breath-by-breath gas exchange. *J. Appl. Physiol.* **89**, 581-589. doi:10.1152/jappl.2000.89.2.581

Fish, F. E. (1993a). Influence of hydrodynamic design and propulsive mode on mammalian swimming energetics. *Aust. J. Zool.* **42**, 79-101. doi:10.1071/ZO9940079

Fish, F. E. (1993b). Power output and propulsive efficiency of swimming bottlenose dolphins (*Tursiops truncatus*). *J. Exp. Biol.* **185**, 179-193. doi:10.1242/jeb.185.1.179

Frid, A. and Dill, L. M. (2002). Human-caused disturbance stimuli as a form of predation risk. *Conserv. Ecol.* **6**, 11. doi:10.5751/ES-00404-060111

Gabaldon, J., Turner, E. L., Johnson-Roberson, M., Barton, K., Johnson, M., Anderson, E. J. and Shorter, K. A. (2019). Integration, calibration, and experimental verification of a speed sensor for swimming animals. *IEEE Sens. J.* **19**, 3616-3625. doi:10.1109/JSEN.2019.2895806

Gleiss, A. C., Wilson, R. P. and Shepard, E. L. C. (2011). Making overall dynamic body acceleration work: on the theory of acceleration as a proxy for energy expenditure. *Methods Ecol. Evol.* **2**, 23-33. doi:10.1111/j.2041-210X.2010.00057.x

Goldbogen, J. A., Cade, D. E., Wisniewska, D. M., Potvin, J., Segre, P. S., Savoca, M. S., Hazen, E. L., Czapanskiy, M. F., Kahane-Rapport, S. R., DeRuiter, S. L. et al. (2019). Why whales are big but not bigger: Physiological drivers and ecological limits in the age of ocean giants. *Science* **366**, 1367-1372. doi:10.1126/science.aax9044

Gorman, M. L., Mills, M. G., Raath, J. P. and Speakman, J. R. (1998). High hunting costs make African wild dogs vulnerable to kleptoparasitism by hyaenas. *Nature* **391**, 479-481. doi:10.1038/35131

Green, J. A. (2011). The heart rate method for estimating metabolic rate: review and recommendations. *Comp. Biochem. Physiol. A Mol. Integr. Physiol.* **158**, 287-304. doi:10.1016/j.cbpa.2010.09.011

Grémillet, D., Lescroël, A., Ballard, G., Dugger, K. M., Massaro, M., Porzig, E. L. and Ainley, D. G. (2018). Energetic fitness: Field metabolic rates assessed via 3D accelerometry complement conventional fitness metrics. *Funct. Ecol.* **32**, 1203-1213. doi:10.1111/1365-2435.13074

Halsey, L. G. (2017). Relationships grow with time: a note of caution about energy expenditure-proxy correlations, focussing on accelerometry as an example. *Funct. Ecol.* **31**, 1176-1183. doi:10.1111/1365-2435.12822

Halsey, L. G. and White, C. R. (2010). Measuring energetics and behaviour using accelerometry in cane toads *Bufo marinus*. *PLoS One* **5**, e10170. doi:10.1371/journal.pone.0010170

Halsey, L. G., Shepard, E. L. C., Quintana, F., Gomez Laich, A., Green, J. A. and Wilson, R. P. (2009). The relationship between oxygen consumption and body acceleration in a range of species. *Comp. Biochem. Physiol. A Mol. Integr. Physiol.* **152**, 197-202. doi:10.1016/j.cbpa.2008.09.021

Halsey, L. G., White, C. R., Enstipp, M. R., Wilson, R. P., Butler, P. J., Martin, G. R., Grémillet, D. and Jones, D. R. (2011a). Assessing the validity of the accelerometry technique for estimating the energy expenditure of diving double-crested cormorants *Phalacrocorax auritus*. *Physiol. Biochem. Zool.* **84**, 230-237. doi:10.1086/658636

Halsey, L. G., Jones, T. T., Jones, D. R., Liebsch, N. and Booth, D. T. (2011b). Measuring energy expenditure in sub-adult and hatchling sea turtles via accelerometry. *PLoS ONE* **6**, e22311. doi:10.1371/journal.pone.0022311

Hertel, H. (1969). Hydrodynamics of swimming and wave-riding dolphins. In *The Biology of Marine Mammals* (ed. H. T. Andersen), pp. 31-63. New York: Academic Press.

Hill, R. W., Wyse, G. A. and Anderson, M. (2012). Energy Metabolism. In *Animal Physiology*, pp. 168-169. Sunderland, MA: Sinauer Associates.

Jeanniard-du-Dot, T., Guinet, C., Arnould, J. P. Y., Speakman, J. R. and Trites, A. W. (2017a). Accelerometers can measure total and activity-specific energy expenditures in free-ranging marine mammals only if linked to time-activity budgets. *Funct. Ecol.* **31**, 377-386. doi:10.1111/1365-2435.12729

Jeanniard-du-Dot, T., Trites, A. W., Arnould, J. P. Y., Speakman, J. R. and Guinet, C. (2017b). Activity-specific metabolic rates for diving, transiting, and resting at sea can be estimated from time-activity budgets in free-ranging marine mammals. *Ecol. Evol.* **7**, 2969-2976. doi:10.1002/ece3.2546

John, J. (2020). Energetics of rest and locomotion in diving marine mammals: novel metrics for predicting the vulnerability of threatened cetacean, pinniped, and sirenian species. *PhD dissertation*, University of California, Santa Cruz.

Johnson, M. P. and Tyack, P. L. (2003). A digital acoustic recording tag for measuring the response of wild marine mammals to sound. *IEEE J. Ocean. Eng.* **28**, 3-12. doi:10.1109/JOE.2002.808212

Karasov, W. H. (1992). Daily energy expenditure and the cost of activity in mammals. *Am. Zool.* **32**, 238-248.

Kéry, M. (2010). *Introduction to WinBUGS for Ecologists: Bayesian Approach to Regression, ANOVA, Mixed Models and Related Analyses*. Academic Press.

King, S. L., Schick, R. S., Donovan, C., Booth, C. G., Burgman, M., Thomas, L. and Harwood, J. (2015). An interim framework for assessing the population consequences of disturbance. *Methods Ecol. Evol.* **6**, 1150-1158. doi:10.1111/2041-210X.12411

Kleiber, M. (1975). *The Fire of Life: An Introduction to Animal Energetics*. New York: Robert E. Krieger Publishing.

Koo, T. K. and Li, M. Y. (2016). A guideline of selecting and reporting intraclass correlation coefficients for reliability research. *J. Chiropr. Med.* **15**, 155-163. doi:10.1016/j.jcm.2016.02.012

Ladds, M. A., Rosen, D. A. S., Slip, D. J. and Harcourt, R. G. (2017). Proxies of energy expenditure for marine mammals: an experimental test of "the time trap". *Sci. Rep.* **7**, 11815. doi:10.1038/s41598-017-11576-4

Maresh, J. L. (2014). Bioenergetics of marine mammals: the influence of body size, reproductive status, locomotion and phylogeny on metabolism. *PhD dissertation*, University of California, Santa Cruz.

Maresh, J. L., Simmons, S. E., Crocker, D. E., McDonald, B. I., Williams, T. M. and Costa, D. P. (2014). Free-swimming northern elephant seals have low field metabolic rates that are sensitive to an increased cost of transport. *J. Exp. Biol.* **217**, 1485-1495. doi:10.1242/jeb.094201

McDonald, B. I., Johnson, M. and Madsen, P. T. (2018). Dive heart rate in harbour porpoises is influenced by exercise and expectations. *J. Exp. Biol.* **221**, jeb168740. doi:10.1242/jeb.168740

Muggeo, V. M. R. (2003). Estimating regression models with unknown break-points. *Stat. Med.* **22**, 3055-3071. doi:10.1002/sim.1545

Nabe-Nielsen, J., van Beest, F. M., Grimm, V., Sibly, R. M., Teilmann, J. and Thompson, P. M. (2018). Predicting the impacts of anthropogenic disturbances on marine populations. *Conserv. Lett.* **11**, e12563. doi:10.1111/conl.12563

Noren, D. P., Holt, M. M., Dunkin, R. C. and Williams, T. M. (2013). The metabolic cost of communicative sound production in bottlenose dolphins (*Tursiops truncatus*). *J. Exp. Biol.* **216**, 1624-1629. doi:10.1242/jeb.083212

Nowacek, D. P., Christiansen, F., Bejder, L., Goldbogen, J. A. and Friedlaender, A. S. (2016). Studying cetacean behaviour: new technological approaches and conservation applications. *Anim. Behav.* **120**, 235-244. doi:10.1016/j.anbehav.2016.07.019

Otani, S., Naito, Y., Kato, A. and Kawamura, A. (2001). Oxygen consumption and swim speed of the harbor porpoise *Phocoena phocoena*. *Fish. Sci.* **67**, 894-898. doi:10.1046/j.1444-2906.2001.00338.x

Pedersen, M. B., Fahlman, A., Borque-Espinosa, A., Madsen, P. T. and Jensen, F. H. (2020). Whistling is metabolically cheap for communicating bottlenose dolphins (*Tursiops truncatus*). *J. Exp. Biol.* **223**, jeb212498. doi:10.1242/jeb.212498

Pirotta, E., Booth, C. G., Costa, D. P., Fleishman, E., Kraus, S. D., Lusseau, D., Moretti, D., New, L. F., Schick, R. S., Schwarz, L. K. et al. (2018). Understanding the population consequences of disturbance. *Ecol. Evol.* **8**, 9934-9946. doi:10.1002/ece3.4458

Qasem, L., Cardew, A., Wilson, A., Griffiths, I., Halsey, L. G., Shepard, E. L. C., Gleiss, A. C. and Wilson, R. (2012). Tri-axial dynamic acceleration as a proxy for animal energy expenditure; should we be summing values or calculating the vector? *PLoS ONE* **7**, e31187. doi:10.1371/journal.pone.0031187

Quanjer, P. H., Tammeling, G. J., Cotes, J. E., Pedersen, O. F., Peslin, R. and Yernault, J.-C. (1993). Lung volumes and forced ventilatory flows. *Eur. Respir. J.* **6**, 5-40. doi:10.1183/09041950.005s1693

Ramsey, F. and Schafer, D. (2013). *The Statistical Sleuth*, 3rd edn. Cengage Learning.

Rimbach, R., Amireh, A., Allen, A., Hare, B., Guarino, E., Kaufman, C., Salomons, H. and Pontzer, H. (2021). Total energy expenditure of bottlenose dolphins (*Tursiops truncatus*) of different ages. *J. Exp. Biol.* **224**, jeb242218. doi:10.1242/jeb.242218

Robson, A. A., Chauvaud, L., Wilson, R. P. and Halsey, L. G. (2012). Small actions, big costs: the behavioural energetics of a commercially important invertebrate. *J. R. Soc. Interface* **9**, 1486-1498. doi:10.1098/rsif.2011.0713

Rohr, J. J., Fish, F. E. and Gilpatrick, J. W., Jr. (2002). Maximum swim speeds of captive and free–ranging delphinids: Critical analysis of extraordinary performance. *Mar. Mammal Sci.* **18**, 1-19. doi:10.1111/j.1748-7692.2002.tb01014.x

Rojano-Doñate, L., McDonald, B. I., Wisniewska, D. M., Johnson, M., Teilmann, J., Wahlberg, M., Højer-Kristensen, J. and Madsen, P. T. (2018). High field metabolic rates of wild harbour porpoises. *J. Exp. Biol.* **221**, jeb185827. doi:10.1242/jeb.185827

Roos, M. M. H., Wu, G. and Miller, P. J. O. (2016). The significance of respiration timing in the energetics estimates of free-ranging killer whales (*Orcinus orca*). *J. Exp. Biol.* **219**, 2066-2077. doi:10.1242/jeb.137513

Scantlebury, D. M., Mills, M. G. L., Wilson, R. P., Wilson, J. W., Mills, M. E. J., Durant, S. M., Bennett, N. C., Bradford, P., Marks, N. J. and Speakman, J. R. (2014). Flexible energetics of cheetah hunting strategies provide resistance against kleptoparasitism. *Science (80-.)*. **346**, 79-81. doi:10.1126/science.1256424

Schmidt-Nielsen, K. (1995). *Animal Physiology Adaption and Environment*, 4th edn. Cambridge University Press.

Schwacke, L. H., Thomas, L., Wells, R. S., McFee, W. E., Hohn, A. A., Mullin, K. D., Zolman, E. S., Quigley, B. M., Rowles, T. K. and Schwacke, J. H. (2017). Quantifying injury to common bottlenose dolphins from the Deepwater Horizon oil spill using an age-, sex- and class-structured population model. *Endanger. Species Res.* **33**, 265-279. doi:10.3354/esr00777

Skinner, J. P., Mitani, Y., Burkanov, V. N. and Andrews, R. D. (2014). Proxies of food intake and energy expenditure for estimating the time-energy budgets of lactating northern fur seals *Callorhinus ursinus*. *J. Exp. Mar. Bio. Ecol.* **461**, 107-115. doi:10.1016/j.jembe.2014.08.002

Skrovan, R. C., Williams, T. M., Berry, P. S., Moore, P. W. and Davis, R. W. (1999). The diving physiology of bottlenose dolphins (*Tursiops truncatus*). II. Biomechanics and changes in buoyancy at depth. *J. Exp. Biol.* **202**, 2749-2761. doi:10.1242/jeb.202.20.2749

Speakman, J. R. (1997). *Doubly-Labelled Water: Theory and Practice*. London: Springer Science and Business Media.

Sumich, J. L. (2021). Why Baja? A bioenergetic model for comparing metabolic rates and thermoregulatory costs of gray whale calves (*Eschrichtius robustus*). *Mar. Mammal Sci.* **37**, 870-887. doi:10.1111/mms.12778

van der Hoop, J. M., Fahlman, A., Hurst, T., Rocho-Levine, J., Shorter, K. A., Petrov, V. and Moore, M. J. (2014). Bottlenose dolphins modify behavior to reduce metabolic effect of tag attachment. *J. Exp. Biol.* **217**, 4229-4236. doi:10.1242/jeb.108225

Villegas-Amtmann, S., Schwarz, L. K. S. and Sumich, J. L. (2015). A bioenergetics model to evaluate demographic consequences of disturbance in marine mammals applied to gray whales. *Ecosphere* **6**, 1-19. doi:10.1890/ES15-00146.1

Wasserman, K., Van Kessel, A. L. and Burton, G. G. (1967). Interaction of physiological mechanisms during exercise. *J. Appl. Physiol.* **22**, 71-85. doi:10.1152/jappl.1967.22.1.71

Williams, T. M., Friedl, W. A. and Haun, J. E. (1993). The physiology of bottlenose dolphins (*Tursiops truncatus*): heart rate, metabolic rate and plasma lactate concentration during exercise. *J. Exp. Biol.* **179**, 31-46. doi:10.1242/jeb.179.1.31

Williams, T. M., Haun, J., Davis, R. W., Fuiman, L. A. and Kohin, S. (2001). A killer appetite: metabolic consequences of carnivory in marine mammals. *Comp. Biochem. Physiol. A Mol. Integr. Physiol.* **129**, 785-796. doi:10.1016/S1095-6433(01)00347-6

Williams, T. M., Fuiman, L. A., Horning, M. and Davis, R. W. (2004). The cost of foraging by a marine predator, the Weddell seal *Leptonychotes weddellii*: pricing by the stroke. *J. Exp. Biol.* **207**, 973-982. doi:10.1242/jeb.00822

Williams, R., Thomas, L., Ashe, E., Clark, C. W. and Hammond, P. S. (2016). Gauging allowable harm limits to cumulative, sub-lethal effects of human activities on wildlife: A case-study approach using two whale populations. *Mar. Policy* **70**, 58-64. doi:10.1016/j.marpol.2016.04.023

Williams, T. M., Kendall, T. L., Richter, B. P., Ribeiro-French, C. R., John, J. S., Odell, K. L., Losch, B. A., Feuerbach, D. A. and Stamper, M. A. (2017). Swimming and diving energetics in dolphins: a stroke-by-stroke analysis for predicting the cost of flight responses in wild odontocetes. *J. Exp. Biol.* **220**, 1135-1145. doi:10.1242/jeb.154245

Williams, T. M., Peter-Heide Jørgensen, M., Pagano, A. M. and Bryce, C. M. (2020). Hunters versus hunted: New perspectives on the energetic costs of survival at the top of the food chain. *Funct. Ecol.* **34**, 2015-2029. doi:10.1111/1365-2435.13649

Wilmers, C. C., Nickel, B., Bryce, C. M., Smith, J. A., Wheat, R. E. and Yovovich, V. (2015). The golden age of bio-logging: how animal-borne sensors are advancing the frontiers of ecology. *Ecology* **96**, 1741-1753. doi:10.1890/14-1401.1

Wilson, R. P., White, C. R., Quintana, F., Halsey, L. G., Liebsch, N., Martin, G. R. and Butler, P. J. (2006). Moving towards acceleration for estimates of activity-specific metabolic rate in free-living animals: the case of the cormorant. *J. Anim. Ecol.* **75**, 1081-1090. doi:10.1111/j.1365-2656.2006.01127.x

Wilson, A. M., Lowe, J. C., Roskilly, K., Hudson, P. E., Golabek, K. A. and McNutt, J. W. (2013). Locomotion dynamics of hunting in wild cheetahs. *Nature* **498**, 185-189. doi:10.1038/nature12295

Wilson, R. P., Börger, L., Holton, M. D., Scantlebury, D. M., Gómez-Laich, A., Quintana, F., Rosell, F., Graf, P. M., Williams, H., Gunner, R. et al. (2020). Estimates for energy expenditure in free–living animals using acceleration proxies: A reappraisal. *J. Anim. Ecol.* **89**, 161-172. doi:10.1111/1365-2656.13040

Withers, P. C. (1977). Measurement of V_{O_2}, V_{CO_2}, and evaporative water loss with a flow-through mask. *J. Appl. Physiol.* **42**, 120-123. doi:10.1152/jappl.1977.42.1.120

Wright, S., Metcalfe, J. D., Hetherington, S. and Wilson, R. (2014). Estimating activity-specific energy expenditure in a teleost fish, using accelerometer loggers. *Mar. Ecol. Prog. Ser.* **496**, 19-32. doi:10.3354/meps10528

Yazdi, P., Kilian, A. and Culik, B. M. (1999). Energy expenditure of swimming bottlenose dolphins (*Tursiops truncatus*). *Mar. Biol.* **134**, 601-607. doi:10.1007/s002270050575

Yeates, L. C. and Houser, D. S. (2008). Thermal tolerance in bottlenose dolphins (*Tursiops truncatus*). *J. Exp. Biol.* **211**, 3249-3257. doi:10.1242/jeb.020610